ELSEVIER

Physica A 266 (1999) 307–311

PHYSICA A

Microstructure analysis of reconstructed porous media

B. Biswal[a,b,*], R. Hilfer[a]

[a] *ICA-1, Universität Stuttgart, Pfaffenwaldring 27, 70569 Stuttgart, Germany*

[b] *Department of Physics and Electronics, Sri Venkateswara College, University of Delhi, New Delhi, 110 021, India*

Abstract

We compare the quantitative microstructural properties of Berea Sandstone with stochastic reconstructions of the same sandstone. The comparison is based on local porosity theory. The reconstructions employ Fourier space filtering of Gaussian random fields and match the average porosity and two-point correlation function of the experimental model. Connectivity properties of the stochastic models differ significantly from the experimental model. Reconstruction models with different levels of coarse graining also show different average local connectivity.

1. Introduction

Recently, a number of stochastic models have been proposed for reconstruction of the microstructure of porous media (see [1,2] and references therein). To assess the quality of the reconstruction, it is neccessary to have quantitative methods of comparison for such microstructures. General geometric characterization methods normally include porosities, specific surface areas and correlation functions [4]. Here we follow a more general quantitative characterization for stochastic microstructures which is based on local porosity theory (LPT) [3,4]. Our analysis allows to distinguish quantitatively between three different microstructures all of which have identical porosities and correlation functions. The three microstructures are an experimental sample of Berea Sandstone obtained by computerized microtomography and two stochastic models of the same sandstone obtained through the Gaussian filtering method [1].

Consider a three-dimensional sample $\mathbb{S}=\mathbb{P}\cup\mathbb{M}$ (with $\mathbb{P}\cap\mathbb{M}=\emptyset$) where $\mathbb{P}$ is the pore space, $\mathbb{M}$ is the rock or mineral matrix. $\emptyset$ denotes is the empty set. The porosity $\phi(\mathbb{S})$

* Corresponding author.

0378-4371/99/$ – see front matter
PII: S0378-4371(98)00607-4

of such a two component porous medium is defined as the ratio $\phi(\mathbb{S}) = V(\mathbb{P})/V(\mathbb{S})$ where $V(\mathbb{P})$ denotes the volume of the pore space, and $V(\mathbb{S})$ is the total sample volume. For the sample data analysed here the set $\mathbb{S}$ is a cube with sidelength M in units of the lattice constant a of a simple cubic lattice. Let $\mathbb{K}(\mathbf{r}, L)$ denote a cube of sidelength L centered at the lattice vector $\mathbf{r}$. The set $\mathbb{K}(\mathbf{r}, L)$ defines a measurement cell inside of which local geometric properties such as porosity and pore space connectivity are measured [3–5]. The *local porosity* in this measurement cell $\mathbb{K}(\mathbf{r}, L)$ is defined as $\phi(\mathbf{r}, L) = [V(\mathbb{P} \cap \mathbb{K}(\mathbf{r}, L))]/[V(\mathbb{K}(\mathbf{r}, L))]$. The *local porosity distribution* $\mu(\phi, L)$ is defined as $\mu(\phi, L) = 1/m \sum_{\mathbf{r}} \delta(\phi - \phi(\mathbf{r}, L))$, where m is the number of placements of the measurement cell $\mathbb{K}(\mathbf{r}, L)$. For better statistics the results presented here are obtained by placing $\mathbb{K}(\mathbf{r}, L)$ on all lattice sites $\mathbf{r}$ which are at least a distance $L/2$ from the boundary of $\mathbb{S}$. The *local percolation probabilities* characterize the connectivity of measurement cells of a given local porosity. Let $\Lambda_\alpha(\mathbf{r}, L)$ equal 1 if $\mathbb{K}(\mathbf{r}, L)$ percolates in "α" direction and 0 otherwise, be an indicator for percolation. A cell $\mathbb{K}(\mathbf{r}, L)$ is called "percolating in the x-direction" if there exists a path inside the set $\mathbb{P} \cap \mathbb{K}(\mathbf{r}, L)$ connecting those two faces of $\mathbb{S}$ that are vertical to the x-axis. Similarly for the other directions. $\Lambda_3 = 1$ indicates that the cell can be traversed along all three directions, while $\Lambda_c = 1$ indicates that there exists at least one direction along which the block is percolating. The local percolation probability in the "α"-direction is defined through $\lambda_\alpha(\phi, L) = [\sum_{\mathbf{r}} \Lambda_\alpha(\mathbf{r}, L)\delta_{\phi\phi(\mathbf{r}, L)}]/[\sum_{\mathbf{r}} \delta_{\phi\phi(\mathbf{r}, L)}]$ and gives the fraction of measurement cells of size L having porosity ϕ that are percolating in the "α"-direction. The *total fraction of percolating cells* which percolate along the "α"-direction is given by $p_\alpha(L) = \int_0^1 \mu(\phi, L)\lambda_\alpha(\phi, L)\,\mathrm{d}\phi$.

The Gaussian field (GF) reconstruction model [1] generates a random pore space configuration with inputs from a given experimental sample. Given the reference correlation function $G_{\mathsf{EX}}(\mathbf{r})$ and porosity $\phi(\mathbb{S}_{\mathsf{EX}})$ of the experimental sample, the three main steps of constructing the sample $\mathbb{S}_{\mathsf{GF}}$ with correlation function $G_{\mathsf{GF}}(\mathbf{r}) = G_{\mathsf{EX}}(\mathbf{r})$ and porosity $\phi(\mathbb{S}_{\mathsf{GF}}) = \phi(\mathbb{S}_{\mathsf{EX}})$ are as follows:

1. A standard Gaussian field $X(\mathbf{r})$ is generated which consists of statistically independent Gaussian random variables $X \in \mathbb{R}$ at each lattice point $\mathbf{r}$.

2. The field $X(\mathbf{r})$ is first passed through a linear filter which produces a correlated Gausssian field $Y(\mathbf{r})$ with zero mean and unit variance.

3. The correlated field $Y(\mathbf{r})$ is then passed through a nonlinear discretization filter which produces the reconstructed sample $\mathbb{S}_{\mathsf{GF}}$.

For the process described in step 2, we have followed an alternate and computationally more efficient method proposed in Ref. [1] that uses Fourier transforms. An effective reconstruction requires a large separation $\xi_{\mathsf{EX}} \ll M$ where M is the sidelength(in pixels) of the sample and ξ_{EX} is the correlation length of the experimental reference, defined as the length such that $G_{\mathsf{EX}}(r) \approx 0$ for $r > \xi_{\mathsf{EX}}$. Violation of this condition leads to inaccuracy in the implementation of step 2 of the reconstruction, which in turn leads to a discrepancy at small r between $G_{\mathsf{GF}}(r)$ and $G_{\mathsf{EX}}(r)$. This problem can be overcome by choosing large M. However, in $d = 3$ very large M also demands prohibitively large memory. Apart from this, the reconstruction also depends

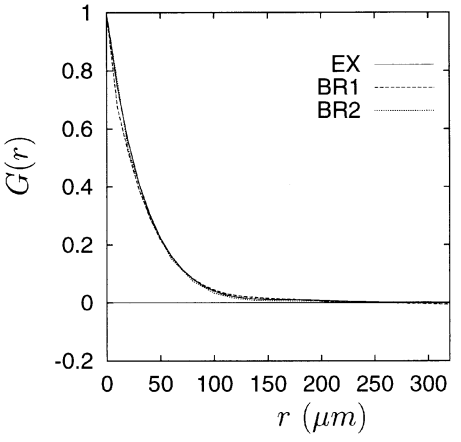

Fig. 1. Averaged directional correlation functions of all three models.

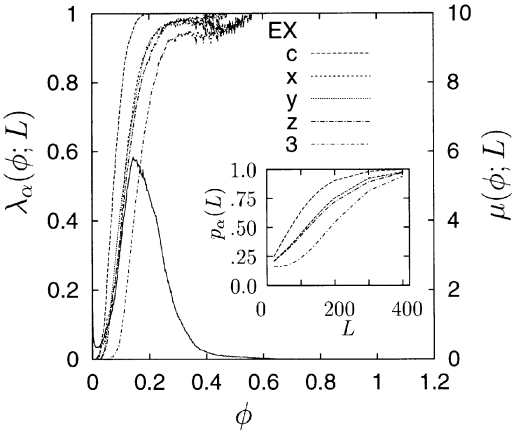

Fig. 2. $\lambda_\alpha(\phi,L)$ (broken curves, left axis) and $\mu(\phi,L)$(solid curve, right axis) at $L=200\,\mu$m for the model EX. The inset shows the function $p_\alpha(L)$, α is given in the legend.

crucially on two other parameters, a length M_c up to which the experimental correlation is incorporated into the reconstructed sample, and n, an interval at which the $G_{\mathsf{EX}}(r)$ is sampled. For better reconstruction $G_{\mathsf{EX}}(M_c)$ needs to be negligibly small. Different values of n correspond to a change of length scale. The model BR1 is constructed with $n=1$ and BR2 with $n=2$. Although both have the same sidelength, the effective size of BR2 is twice that of BR1 because of this coarse graining procedure.

In Fig. 1 the averaged correlation functions $G(r)=(G(r,0,0)+G(0,r,0)+G(0,0,r))/3$ for the three samples are plotted. The experimental sample is a Berea sandstone of porosity $\phi(\mathbb{S}_{\mathsf{EX}})=0.1775$ [5]. The model BR1, with $M=128$, $n=1$ and $M_c=32$, shows descrepancies for small values of r. However, for BR2, with $M=128$, $n=2$ and $M_c=32$, the correlation function matches more closely to that of EX. The resolution

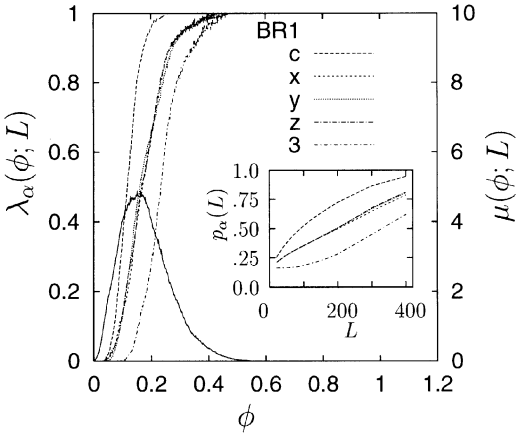

Fig. 3. $\lambda_\alpha(\phi, L)$ (broken curves, left axis) and $\mu(\phi, L)$(solid curve, right axis) at $L = 200\,\mu$m for the model BR1. The inset shows the functions $p_\alpha(L)$, α is given in the legend.

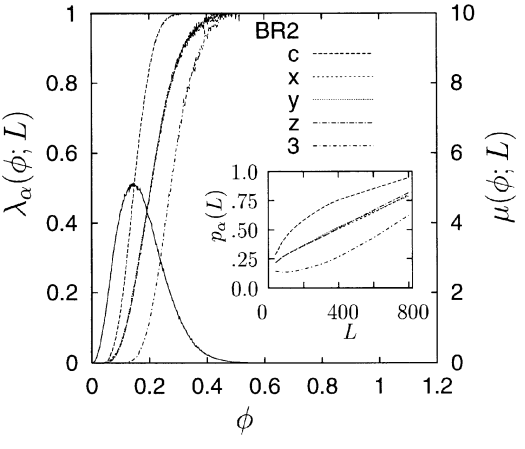

Fig. 4. $\lambda_\alpha(\phi, L)$ (broken curves, left axis) and $\mu(\phi, L)$(solid curve, right axis) at $L = 200\,\mu$m for the model BR2. The inset shows the functions $p_\alpha(L)$, α is given in the legend.

a of the experimental sample EX is 10 μm. Hence the actual size of EX and BR1 is 1280 μm, whereas that of BR2 is 2560 μm. The porosities match quite well for all the samples ($\phi(\mathbb{S}_{\mathrm{BR1}}) = 0.1783$ and $\phi(\mathbb{S}_{\mathrm{BR2}}) = 0.1776$).

The reconstructed models BR1 and BR2 are isotropic and globally connected, i.e., the pore spaces percolate in all the three directions. The local porosity analysis results are plotted in Fig. 2 for the experimental sample EX, in Fig. 3 for the stochastic model BR1, and in Fig. 4 for BR2. Comparison of $\mu(\phi, L)$ indicates that the stochastic models have nearly the same level of homogeneity with that of the experimental sample. The main differences are found in $\lambda_\alpha(\phi, L)$ of the stochastic models. They differ significantly from that of EX, and they also vary widely among themselves. The

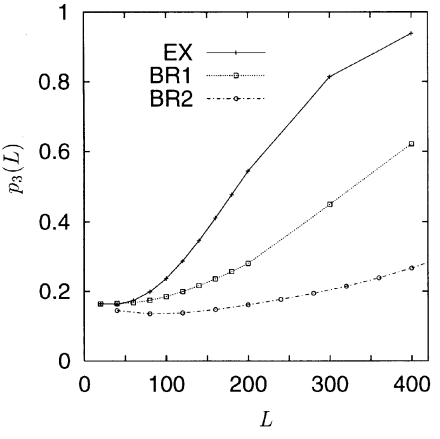

Fig. 5. $p_3(L)$ for the three samples.

reconstructed models have lower average connectivity of pore spaces. We observe $[\lambda_\alpha(\phi,L)]_{\mathsf{EX}} > [\lambda_\alpha(\phi,L)]_{\mathrm{BR1}} > [\lambda_\alpha(\phi,L)]_{\mathrm{BR2}}$. These differences appear even more clearly in the plot of $p_\alpha(L)$ (inset of Figs. 2–4). In the experimental model (Fig. 2) nearly all the measurement cells of dimension larger than 400 μm are percolating (globally connected pore space) in all directions. Comparison of $p_3(L)$ of the three models (Fig. 5) shows the drastic loss of average connectivity of the reconstructed models. Fig. 5 shows that the GF reconstruction BR1 with $n=1$ has a lower connectivity than EX. In BR1 nearly 60% of the measurement cells of size 400 μm percolate in all directions. Coarse graining [1] to $n=2$ further reduces the connectivity of pore space. In BR2 less than 30% of the measurement cells of size 400 μm percolate in all directions. These results indicate that Gaussian filtering reconstruction methods retain a similar degree of isotropy and homogeneity as the original sandstone but tend not to reproduce connectivity properties that are important for transport.

References

[1] P. Adler, Porous Media, Butterworth-Heinemann, Boston, 1992.
[2] C. Yeong, S. Torquato, Reconstructing random media, Phys. Rev. E 57 (1998) 495–506.
[3] R. Hilfer, Local porosity theory for flow in porous media, Phys. Rev. B 45 (1992) 7115–7121.
[4] R. Hilfer, Transport and relaxation phenomena in porous media, Adv. Chem. Phys. XCII (1996) 299–424.
[5] B. Biswal, C. Manwart, R. Hilfer, Three-dimensional local porosity analysis of porous media, Physica A 255 (1998) 221–241.